

High efficiency electrophosphorescence device using a thin cleaving layer in an Ir-complex doped emitter layer

Dongfang Yang, Wenlian Li, Bei Chu, Dongyu Zhang, Jianzhuo Zhu et al.

Citation: *Appl. Phys. Lett.* **92**, 253309 (2008); doi: 10.1063/1.2952954

View online: <http://dx.doi.org/10.1063/1.2952954>

View Table of Contents: <http://apl.aip.org/resource/1/APPLAB/v92/i25>

Published by the [American Institute of Physics](#).

Related Articles

Inverted top-emitting blue electrophosphorescent organic light-emitting diodes with high current efficacy
APL: Org. Electron. Photonics **5**, 202 (2012)

Inverted top-emitting blue electrophosphorescent organic light-emitting diodes with high current efficacy
Appl. Phys. Lett. **101**, 103304 (2012)

Degradation induced decrease of the radiative quantum efficiency in organic light-emitting diodes
APL: Org. Electron. Photonics **5**, 199 (2012)

Degradation induced decrease of the radiative quantum efficiency in organic light-emitting diodes
Appl. Phys. Lett. **101**, 103301 (2012)

High-efficiency organic light-emitting diodes utilizing thermally activated delayed fluorescence from triazine-based donor-acceptor hybrid molecules
Appl. Phys. Lett. **101**, 093306 (2012)

Additional information on *Appl. Phys. Lett.*

Journal Homepage: <http://apl.aip.org/>

Journal Information: http://apl.aip.org/about/about_the_journal

Top downloads: http://apl.aip.org/features/most_downloaded

Information for Authors: <http://apl.aip.org/authors>

ADVERTISEMENT



HAVE YOU HEARD?

Employers hiring scientists
and engineers trust
physicstodayJOBS

<http://careers.physicstoday.org/post.cfm>



High efficiency electrophosphorescence device using a thin cleaving layer in an Ir-complex doped emitter layer

Dongfang Yang, Wenlian Li,^{a)} Bei Chu,^{a)} Dongyu Zhang, Jianzhuo Zhu, Zisheng Su, Wenming Su, Liangliang Han, Defeng Bi, Yiren Chen, Fei Yan, Huihui Liu, and Dan Wang
Key Laboratory of Excited State Processes, Changchun Institute of Optics, Fine Mechanics and Physics, Chinese Academy of Sciences, Changchun 130033, People's Republic of China
and Graduate School of Chinese Academy of Sciences, Beijing 100039, People's Republic of China

(Received 13 December 2007; accepted 22 May 2008; published online 27 June 2008)

The authors demonstrate a considerable increase in current efficiency of fac-tris(2-phenylpyridine) iridium doped phosphorescent organic green-light emitting diode in which a thin 4,7 dipheny-1,10-phenanthroline (Bphen) layer acts as a cleaving layer. As 4 nm Bphen layer divides the emitting layer (EML) into two sub-EMLs, a maximum current efficiency of 53 cd/A (corresponding to external efficiency quantum of 15%) is obtained, which is higher for 2.3 folds than that of the device without it, especially the current efficiency increases 64% over the reference device at a luminance of 40 000 cd/m². The increases are demonstrated to the high electron mobility and special energy level alignment of Bphen with 4,4'-N,N'-dicarbazole-biphenyl host. The efficiency improvement attributes to a higher exciton formation probability in the recombination zone and better balance of the carrier injection. The detail enhancement mechanism of the efficiency is also discussed. © 2008 American Institute of Physics. [DOI: 10.1063/1.2952954]

Since Tang and Vanslyke demonstrated organic light emitting diodes (OLEDs) based on fluorescent tris-(8-hydroxy-quinoline) aluminum (Alq₃),¹ a great deal of progress has been made on obtaining high electroluminescence (EL) performances due to uses of both the singlet and triplet excitons. A maximum internal efficiency of 100% of phosphorescence (Ph) devices could be harvested in which fac-tris(2-phenylpyridine) iridium [Ir(ppy)₃] and platinum octaethylporphyrin are adopted as the green and red emitting dopants in 4,4'-N,N'-dicarbazole-biphenyl (CBP) host, respectively, with a bipolar carrier transport property.²⁻⁴

There are many efficient ways of harvesting high EL efficiency such as balancing carrier injection in the emitting layer (EML) and increasing the utilization rate of the exciton.⁵⁻⁸ Chin and Suh used stepwise doping profile to adjust carrier transport in EML to improve the efficiency.⁵ Double EML structures have been reported which were used to reduce the losses of exciton migration into undoped regions and increase the width of the recombination zone.^{6,7} The use of a quantum well structure could also enhance the efficiency of PhOLEDs.⁸ Although above techniques can increase the EL efficiency, there is still space for improving the EL performance, such as enhancing the probability of exciton formation which would be a promising method. The maximum EL efficiency generated by the recombination of oppositely charged carriers injected from the electrodes in OLEDs can be achieved by minimizing the leakages of holes and electrons. This concept inspires us to develop highly efficient OLEDs composed of multiemitting layers, where the internal interfaces act as energy barriers accumulating charge carriers to enhance the probability of exciton formation and decrease the injection of hole from the anode.⁹

Because 4,7 dipheny-1,10-phenanthroline (Bphen) has a low highest occupied molecular orbital (HOMO) level and high electron mobility, it was generally used as an efficient hole blocking and electron transporting (ET) material in OLED devices. In this letter, we use a 4 nm Bphen layer to insert into the 30 nm EML which is divided into two sub-EMLs to design a high efficient Ir-complex based PhOLED. Finally, a maximum current efficiency of 53 cd/A corresponding to an external efficiency quantum of 15% is obtained, which is higher for 2.3 folds than that of the device without it. The increase attributes to two impactful exciton formation zones and better balance of the carrier injection in the two sub-EMLs.

The fabricated PhOLED with structures of indium tin oxide ITO/2-TNATA (10 nm)/4,4'-bis[N-(1-naphthyl)-N-phenyl-amino]-biphenyl (NPB) (25 nm)/[CBP:Ir(ppy)₃]_A (6 wt %, x nm)/Bphen (y nm)/[CBP:Ir(ppy)₃]_B (6 wt %, 30-x nm)/BCP (10 nm)/Alq₃ (15 nm)/LiF (0.5 nm)/Al (120 nm) (see Fig. 1), ([CBP:Ir(ppy)₃]_A and [CBP:Ir(ppy)₃]_B are called as [C:Ir]_A and [C:Ir]_B, respectively, hereafter) in which the total thickness of the [C:Ir]_A

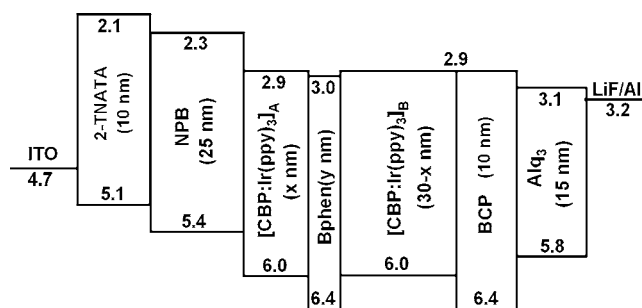


FIG. 1. The device structure of ITO/2-TNATA (10 nm)/NPB (25 nm)/[C:Ir]_A (6 wt %, x nm)/Bphen (y nm)/[C:Ir]_B (6 wt %, 30-x nm)/BCP (10 nm)/Alq₃ (15 nm)/LiF (0.5 nm)/Al (120 nm) and the proposed energy level diagram.

^{a)} Author to whom correspondence should be addressed. Electronic addresses: wllioel@yahoo.com.cn and beichu@163.com.

TABLE I. The current efficiency as a function of the $[\text{CBP}:\text{Ir}(\text{ppy})_3]_{\text{A}}$ layer thickness and the Bphen layer thickness in the EML of the devices.

Thickness (<i>x</i>) of the $[\text{CBP}:\text{Ir}(\text{ppy})_3]_{\text{A}}$ layer (nm)	Thickness (<i>y</i>) of the Bphen layer (nm)	Current efficiency of the devices (cd/A)
30	0	23
20	2	33
20	3	44
20	4	47
20	6	37
5	4	41
10	4	53
20	4	47
25	4	35

and the $[\text{C}:\text{Ir}]_{\text{B}}$ layers was fixed at 30 nm, then the thickness (*x*) of the $[\text{C}:\text{Ir}]_{\text{A}}$ layer and the thickness (*y*) of Bphen layer were changed from 5 to 25 nm and from 0 to 6 nm, respectively. For comparison, another OLED with *x*=30 and *y*=0, i.e., ITO/2-TNATA (10 nm)/NPB (25 nm)/CBP:Ir(ppy)₃ (6 wt %, 30 nm)/BCP (10 nm)/Alq₃ (15 nm)/LiF (0.5 nm)/Al (120 nm) (called as the reference device hereafter) was also prepared, where 2-TNATA and BCP denote 4,4'-bis[2-naphthyl(phenyl)-amino] triphenylamine and 2,9-dimethyl-4,7-diphenyl-1,10-phenanthroline, working as the hole injection layer and hole blocking layer, respectively.

Figure 1 shows the device structure and the schematic energy level diagram, where the lowest unoccupied molecular orbital and the HOMO levels were respectively cited from literature.¹⁰⁻¹³

The PhOLEDs were fabricated using precleaned ITO glass (25 Ω/sq) by thermal evaporation at a base pressure of 3×10^{-4} Pa, followed by a LiF buffer and an Al cathode layers in the same vacuum run. The deposition rates and thickness of all layers were monitored *in situ* using an oscillating quartz monitor. The evaporating rates were kept at 1–2 Å/s for the organic layers and the LiF layer and at 10 Å/s for the Al cathode, respectively. EL spectra of these devices were measured with a Hitachi F-4500 fluorescence spectrophotometer. The luminance-current-voltage (*L-I-V*) characteristics of OLEDs were measured with a 3645 dc power supply combined with a 1980a spot photometer and were recorded simultaneously. All the measurements were carried out at room temperature under ambient conditions.

To optimize the device structure the best combination of *x* nm $[\text{C}:\text{Ir}]_{\text{A}}$ and *y* nm Bphen layer must be found. First, fixing on a 20 nm $[\text{C}:\text{Ir}]_{\text{A}}$, the *y* value was variously changed and then basing on the result, the *x* value was optimized. When *x*=10 nm and *y*=4 nm, the maximum current efficiency is obtained which is as shown in Table I. From Table I we can see that as the Bphen layer thickness increases from 0 to 4 nm, the current efficiency increases, while as the thickness of Bphen increase from 4 to 6 nm, the current ef-

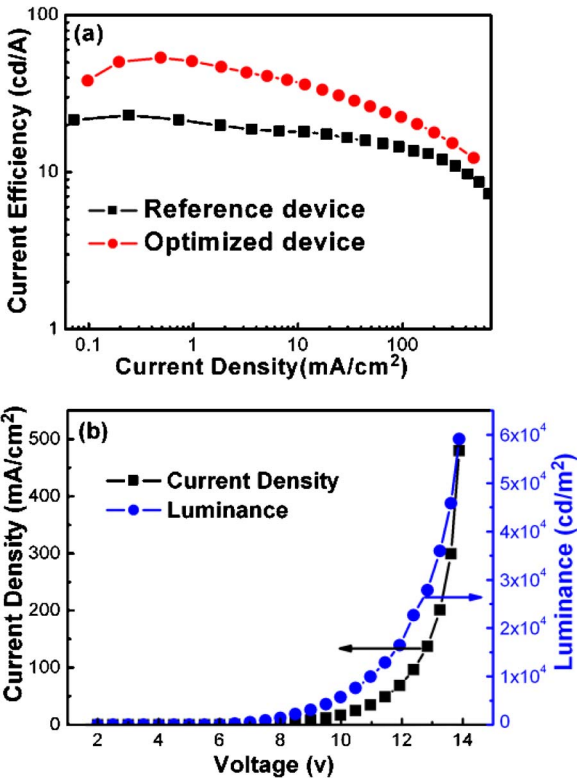


FIG. 2. (Color online) The current efficiency as a function of the current density of the optimized and reference devices (a) and *L-I-V* curves of the optimized device (b).

iciency decreases. When the proper thickness of Bphen layer is found, an optimal hole and electron ratios present in the $[\text{C}:\text{Ir}]_{\text{A}}$ and $[\text{C}:\text{Ir}]_{\text{B}}$ layers. If Bphen layer is too thin or too thick, large part of exciton would be formed in one sub-EML leading to lower efficiency. Furthermore, the thickness ratio between $[\text{C}:\text{Ir}]_{\text{A}}$ and $[\text{C}:\text{Ir}]_{\text{B}}$ layers can also affect the exciton ratio in two sub-EMLs. As a result an optimized device with a structure of ITO/2-TNATA (10 nm)/NPB (25 nm)/ $[\text{CBP}:\text{Ir}(\text{ppy})_3]_{\text{A}}$ (6 wt %, 10 nm)/Bphen (4 nm)/ $[\text{CBP}:\text{Ir}(\text{ppy})_3]_{\text{B}}$ (6 wt %, 20 nm)/BCP (10 nm)/Alq₃ (15 nm)/LiF (0.5 nm)/Al (120 nm) was fabricated. Figure 2(a) shows the current efficiency as a function of the current density for the optimized and reference devices. Table I exhibits the current efficiency as a function of the $[\text{CBP}:\text{Ir}(\text{ppy})_3]_{\text{A}}$ layer thickness and the Bphen layer thickness in the EML of the devices. From Fig. 2(a) and Table I we can see that the optimized device exhibits a maximum current efficiency of 53 cd/A, which increases about 2.3 folds over the reference device. Table II shows the relation between current efficiency and luminance of the optimized device and the reference device. It indicates that even at a luminance of 40 000 cd/m², the efficiency of the optimized device is still higher than that of the reference

TABLE II. The relationship between current efficiency and luminance of the optimized device and the reference device.

Luminance (cd/m²)	50	100	260	500	1000	5000	10 000	20 000	40 000
Reference device current Efficiency (cd/A)	23	22	21	20	18	16.6	15.1	13.5	9.7
Optimized device current Efficiency (cd/A)	40	50	53	51	46	35	28.4	23	16

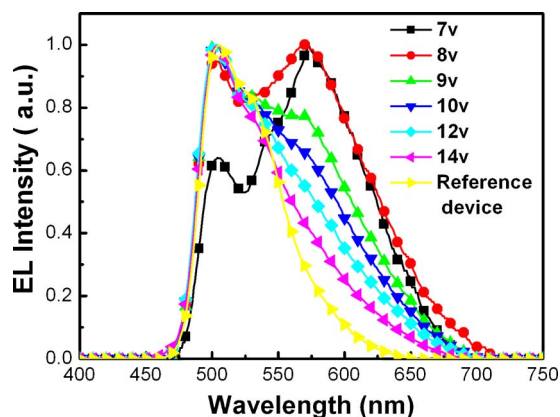


FIG. 3. (Color online) The relationship between the EL emission spectra and the bias of the device with structure of ITO/2-TNATA(10 nm)/NPB (25 nm)/CBP:Ir(ppy)₃ (10 nm)/Bphen (y nm)/CBP:DCJTb (20 nm)/BCP (10 nm)/Alq₃ (15 nm)/LiF (0.5 nm)/Al (120 nm) and the EL spectra of the reference device at 9V.

device by 64%. The maximum luminance of the optimized device is over 60 000 cd/m², as shown in Fig. 2(b).

To probe the exciton distribution in the devices, a device with a structure of ITO/NPB (25 nm)/CBP:Ir(ppy)₃ (10 nm)/Bphen (4 nm)/CBP:4-(dicyanomethylene)-2-*t*-butyle-6-(1,1,7,7-tetramethyljulolidyl-9-enyl)-4*H*-pyran(DCJTb) (20 nm)/BCP (10 nm)/Alq₃ (15 nm)/LiF (0.5 nm)/Al (120 nm) was fabricated. Figure 3 depicts the relationship between the EL emission spectra and the bias of the device. It is noticed the emission of stronger orange-red peak at 571 nm resulted from DCJTb and the weaker green peak at 505 nm from Ir(ppy)₃ at low bias voltage. As the bias increases, the EL color changes from orange red with weaker green to green with orange red. Finally main green emission occurs at bias larger than 14 V. The finding indicates that both of the two EMLs contribute to the whole EL emission. Moreover, this also implies that the inserted Bphen could block holes and the carrier recombination occurs in either CBP:Ir(ppy)₃ layer and the CBP: DCJTb layer, and as the voltage gradually increases, the emission position was moved forward to the anode.^{14,15}

Due to the action of the thin Bphen layer, exciton can format in both the two subregions, i.e., CBP:Ir(ppy)₃ and CBP:DCJTb layers, which could balance the exciton distribution in the two zones. This leads to an increase in recombination probability of carriers in EML. Figure 2(a) indicates that during 0.1 and 0.5 mA/cm² the current efficiency increases gradually with the increases in current density, and then the efficiency falls after 0.5 mA/cm², while the reference device offers lower efficiency throughout the entire driving current region. From the schematic level diagram shown in Fig. 1, we can conclude that the HOMO level of Bphen layer is lower than that of CBP, so a hole injection barrier appears, by which the holes would be piled up in the [C:Ir]_A layer near to the interface between the [C:Ir]_A/Bphen layers. Due to high hole mobility of NPB (Ref. 16) and the thin Bphen layer, the holes can partially penetrate into Bphen layer and reach the [C:Ir]_B layer, which allows the fine tuning of the carrier distribution and the balancing of the carrier injection in the two sub-EMLs. Because Bphen has a high electron mobility of 10⁻⁴ cm²/V s order¹⁷

and a small electron injection barrier between the CBP/Bphen layers, electrons in the [C:Ir]_B layer were transported to the [C:Ir]_A layer and then electrons recombine with the holes in the [C:Ir]_A layer. This leads to an increase in the probability of radiative recombination between the holes and electrons since the recombination can take place in both of the two sub-EMLs. However, electrons with higher density locate at the [C:Ir]_B layer rather than at the [C:Ir]_A layer at low current density, thus the recombination zone would occur mainly in the [C:Ir]_B layer.

At a current density of 0.5 mA/cm², the electron mobility further increases and the electrons in the [C:Ir]_A layer recombine with the holes.¹⁸ As a result, both the two sub-EMLs offer the EL emissions with an optimal emission ratio, leading to the maximum EL efficiency. At the current densities higher than 0.5 mA/cm², the EL emission again results mainly from the [C:Ir]_A layer because the emission position was moved forward to the anode as the voltage increases, so that the EL efficiency gradually decreases as the current density increases. At the same time, the triplet-triplet annihilation is another significant factor for reducing efficiency at high current density.¹⁹ Even now, the efficiency of the optimized device is higher than that of the reference device over the whole current density.

In summary, an improvement of the EL intensity is demonstrated by designing a PhOLED structure in which the EML is cleaved by a 4 nm Bphen layer into two sub-EMLs. At current density of about 0.5 mA/cm², a maximum current efficiency of 53 cd/A is achieved, which is larger than that of the reference device by 2.3 folds and current efficiency increased under whole current density. We attribute this enhancement to the formation of two high efficient exciton formation zones and better balance of the carrier injection in the two sub-EMLs of the PhOLED due to the special HOMO level structure and high ET ability of Bphen material. The use of a Bphen insert layer in a wide EML is expected to simplify the device fabrication of highly efficient PhOLEDs and to design other PhOLED and organic electronic devices.

- ¹C. W. Tang and S. A. VanSlyke, *Appl. Phys. Lett.* **51**, 913 (1987).
- ²M. A. Baldo, D. F. O'Brien, Y. You, A. Shoustikov, S. Sibley, M. E. Thompson, and S. R. Forrest, *Nature (London)* **395**, 151 (1998).
- ³M. A. Baldo, S. Lamansky, P. E. Burrows, M. E. Thompson, and S. R. Forrest, *Appl. Phys. Lett.* **75**, 4 (1999).
- ⁴H. Kanai, S. Ichinosawa, and Y. Sato, *Synth. Met.* **91**, 195 (1997).
- ⁵B. D. Chin and M. C. Suh, *Appl. Phys. Lett.* **86**, 133505 (2005).
- ⁶X. Zhou, D. S. Qin, and K. Leo, *Appl. Phys. Lett.* **81**, 4070 (2002).
- ⁷T. H. Zheng and W. C. H. Choy, *J. Phys. D: Appl. Phys.* **41**, 055103 (2008).
- ⁸S. H. Kim, J. Jang, and J. Y. Lee, *Appl. Phys. Lett.* **90**, 173501 (2007).
- ⁹C. W. Tang, S. A. Van Slyke, and C. H. Chen, *J. Appl. Phys.* **65**, 3610 (1989).
- ¹⁰G. He, M. Pfeiffer, and K. Leo, *Appl. Phys. Lett.* **85**, 3911 (2004).
- ¹¹D. Y. Zhang, W. L. Li, and B. Chu, *Appl. Phys. Lett.* **91**, 183516 (2007).
- ¹²M. A. Baldo and S. R. Forrest, *Phys. Rev. B* **62**, 10958 (2000).
- ¹³K. Okumoto and Y. Shirota, *J. Lumin.* **87**, 1171 (2000).
- ¹⁴C. H. Chen and H. F. Meng, *Appl. Phys. Lett.* **86**, 201102 (2006).
- ¹⁵J. W. Kang and J. J. Kim, *Appl. Phys. Lett.* **90**, 223508 (2007).
- ¹⁶T. Y. Chu and O. K. Song, *Appl. Phys. Lett.* **90**, 203512 (2007).
- ¹⁷S. Naka and H. Onnagawa, *Appl. Phys. Lett.* **76**, 197 (2000).
- ¹⁸L. Bozano, S. A. Carter, J. C. Scott, and P. J. Brock, *Appl. Phys. Lett.* **74**, 1132 (1999).
- ¹⁹M. A. Baldo, C. Adachi, and S. R. Forrest, *Phys. Rev. B* **62**, 10967 (2000).